

Hemostasis, Thrombosis, and vascular biology

Word counts: 4635

**Soluble HLA-G1 inhibits angiogenesis through an apoptotic pathway and by direct binding to CD160 receptor expressed by endothelial cells**

**Pierre Fons, Sophie Chabot, Judith E. Cartwright, Françoise Lenfant, Fatima L'Faqih, Jérôme Giustiniani, Jean-Pascal Herculat, Geneviève Gueguen, Françoise Bono, Pierre Savi, Maryse Aguerre-Girr, Sylvie Fournel, François Malecaze, Armand Bensussan, Jean Plouët, and Philippe Le Bouteiller**

**Short Title:** Soluble HLA-G1 inhibits angiogenesis

From the Institut de Pharmacologie et Biologie Structurale, Centre National de la Recherche Scientifique Unité Mixte de Recherche 5089, Toulouse, France; Sanofi-Aventis Research, Toulouse, France; the Institut National de la Santé et de la Recherche Médicale Unité 563/Université Paul Sabatier, Hôpital Purpan, Toulouse, France; Department of Basic Medical Sciences, St. George's, University of London, United Kingdom; Institut National de la Santé et de la Recherche Médicale Unité 659, Faculté de Médecine de Créteil, Créteil, France; Institut National de la Santé et de la Recherche Médicale Unité 689, Institute des Vaisseaux et du Sang, Paris, France

Philippe Le Bouteiller, Jean Plouët and Armand Bensussan are co-senior authors. Sophie Chabot and Judith E. Cartwright contributed equally to this work.

Supported by a CIFRE-AbTECH fellowship (PF), Institut National de la Santé et de la Recherche Médicale (PLB, AB, JP), Université Paul Sabatier de Toulouse (PLB), the Ligue Nationale contre le Cancer (JP), the Association pour la Recherche sur le Cancer (JP, AB), the British Heart Foundation (JEC), Organon (JT), the Etablissement Français des Greffes (PLB), the Ligue Régionale contre le Cancer, Comités Départements Ariège and Haute Garonne (PLB), and Comité Paris (AB, JP), and the European Union Network of Excellence EMBIC (LSHM-CT-2004-512040) (PLB).

**Reprints:** Philippe Le Bouteiller, INSERM U563, Bat A, Hopital Purpan, BP3028, 31024 Toulouse Cedex 3, France; e-mail: [philippe.le-bouteiller@toulouse.inserm.fr](mailto:philippe.le-bouteiller@toulouse.inserm.fr)

## Abstract

**HLA-G is a Major Histocompatibility Complex class Ib molecule whose constitutive tissue distribution is mainly restricted to trophoblast cells at the maternal-fetal interface during pregnancy. In this study we demonstrate the ability of the soluble HLA-G1 (sHLA-G1) isoform to inhibit fibroblast growth factor-2 (FGF2)-induced capillary-like tubule formation. Using a rabbit corneal neovascularization model, we further show that sHLA-G1 inhibits FGF2-induced angiogenesis *in vivo*. We have also demonstrated that sHLA-G1 induces endothelial cell apoptosis through binding to BY55/CD160, a glycosylphosphatidylinositol-anchored receptor expressed by endothelial cells. Furthermore, we show that the specific CL1-R2 anti-CD160 monoclonal antibody mimics sHLA-G1-mediated inhibition of endothelial cell tube formation and induction of apoptosis. Thus, engagement of CD160 in endothelial cells may be essential for the inhibition of angiogenesis. sHLA-G1/CD160-mediated anti-angiogenic property may participate in the vascular remodeling of maternal spiral arteries during pregnancy, and offers an attractive therapeutic target to prevent pathologic neovascularization as we found that CD160 is strongly expressed in the vasculature of a murine tumor.**

## Introduction

HLA-G is a major human (MHC) histocompatibility class Ib gene characterized by a unique promoter region, limited polymorphism, restricted constitutive tissue distribution and the occurrence of several spliced transcripts encoding either membrane-bound or soluble proteins.<sup>1</sup> The soluble HLA-G1 (sHLA-G1) isoform derives from mRNA retaining intron 4,<sup>2</sup> which contains a stop codon that precludes translation of the transmembrane domain. Such intron 4 retention is unique among all HLA class I molecules described to date. This 37 kDa intron 4-retaining sHLA-G1 isoform associates non covalently with  $\beta$ 2-microglobulin ( $\beta$ 2m).<sup>2</sup> Soluble HLA-G can also be generated by metalloproteinase-mediated release of surface HLA-G containing only extracellular domains.<sup>3</sup> The predominant expression of sHLA-G1 in the placenta at a time when polymorphic HLA-A and HLA-B class Ia molecules are repressed is consistent with important immunological functions during pregnancy.<sup>4</sup> sHLA-G1 induces apoptosis of activated CD8<sup>+</sup> T and NK cells<sup>5,6</sup> and down-regulates CD4<sup>+</sup> T cell allo-proliferation response.<sup>7</sup> The observation that some anti-HLA-G monoclonal antibodies bound to HLA-G negative placental endothelial cells<sup>8,9</sup> led to our hypothesis that sHLA-G1 might bind to these cells and be involved in the modulation of placental angiogenesis and/or uterine vessel remodeling.<sup>8</sup> Several further observations are in line with such a novel function of HLA-G: first, a defect of HLA-G expression in extravillous cytotrophoblast is associated with preeclampsia,<sup>10,11</sup> a common complication of pregnancy in which HLA-G<sup>+</sup> endovascular trophoblast invasion of maternal spiral arteries is abrogated, compromising blood flow to the maternal interface,<sup>12</sup> second, it has been shown that HLA-G inhibits the transendothelial migration of NK cells<sup>13</sup> and the rolling adhesion of activated NK cells on endothelial cells.<sup>14</sup> To date, the potential role of sHLA-G1 in the modulation of angiogenesis has not been addressed.

Angiogenesis, the formation of new capillaries from preexisting blood vessels, is a crucial component of embryonic vascular development and differentiation, wound healing, and organ regeneration.<sup>15</sup> It also contributes to the progression of pathologies that depend on neovascularization, including tumor growth, ischemic ocular disease, and rheumatoid arthritis. While the most important mediators of angiogenesis, the vascular endothelial growth factor (VEGF) and the fibroblast growth factor (FGF)

families are well defined,<sup>16</sup> angiogenesis exists as a complex process involving multiple gene products expressed by different cell types, all contributing to an integrated sequence of events.<sup>17,18</sup>

To test our hypothesis that sHLA-G1 is a regulator of endothelial cell activity, we first investigated its *in vitro* effect. This study demonstrates that sHLA-G1 inhibits FGF-2 or VEGF-induced angiogenesis and triggers apoptosis of endothelial cells by interaction with the glycosylphosphatidylinositol (GPI)-anchored CD160 receptor<sup>19,20</sup> expressed on endothelial cells. Moreover, *in vivo*, sHLA-G1 abolishes angiogenesis. Interestingly, we show by immunohistochemistry performed *ex vivo* that CD160 is expressed solely at the vascular level in a mouse tumor model.

## Materials and methods

### Cells and reagents

Human umbilical vein endothelial cells (HUVEC, Tebu, Le Perray-en-Yvelines, France) and human microvascular endothelial cells (HMVEC) (Cambrex, San Diego, CA) were maintained in EBM (Cambrex) supplemented with 5% fetal calf serum (FCS) and 1 ng/mL FGF2 or VEGF-A 165 (R & D systems, Minneapolis, IL) every other day. SGHEC-7 cells, a HUVEC-derived cell line, and SGHPL-4 extravillous trophoblast cells were cultured as previously described.<sup>21,22</sup> Human aortic smooth muscle cells (HAOSMC) (Cambrex) were maintained in RPMI supplemented with 10% FCS. Primary human fibroblast were obtained from skin biopsies of healthy subjects and grown in Dulbecco modified Eagle medium (DMEM) containing 10% FCS. Human Jurkat T cells and Jurkat transfected with CD160 (Jurkat-CD160) have been previously described.<sup>23</sup> NK92 is a human NK cell line expressing CD160.<sup>23</sup> CD4<sup>+</sup> T cells were purified from human peripheral blood mononuclear cells using the MACS separation system (Miltenyi Biotec, Auburn, CA). The B-lymphoblastoid cell line 721.221-sHLA-G1, a gift from Dr D. Geraghty (Fred Hutchinson Cancer Research Center, Seattle, WA), was obtained by transfection of the intron 4 containing sHLA-G1 cDNA, as described.<sup>2</sup> The resulting transfected protein corresponds to the sHLA-G1 heavy chain non covalently associated to the endogenous  $\beta$ 2m. The sHLA-G1- $\beta$ 2m fusion monochain (sHLA-G1mono) construct was engineered by connecting the last residue of the  $\alpha$ 3 domain of HLA-G to the first codon of the human  $\beta$ 2m sequence through a 15-residue spacer.<sup>24</sup> sHLA-G1mono was transfected in the HLA class I negative trophoblast-derived cell line JAR.<sup>24</sup> Recombinant sHLA-G1 and sHLA-G1mono

molecules were purified from the corresponding transfectant cell culture supernatants by W6/32 monoclonal antibody (mAb) immunoaffinity column, and eluted at basic pH as described.<sup>24</sup> Positive fractions evaluated by HLA-G specific ELISA were pooled, concentrated and analyzed either by SDS-PAGE stained with Coomassie blue or by Western blot using HLA-G specific mAb<sup>24</sup> (Supplementary Figure 1). Monoclonal antibodies used included CL1-R2 (IgG1) anti-CD160,<sup>23</sup> produced in one of our laboratories, anti-CD8 (OKT8, Coulter Immunotech), anti-ILT4/CD85d (gift from Dr M. Colonna, Washington University), anti-ILT2/CD85j (BD Biosciences, San Jose, CA), and dialyzed mouse IgG1 or IgG2a isotype controls (DAKO, Trappes, France). HLA-G1 tetramers were produced as previously described,<sup>25</sup> using synthetic self-peptide RIIPRHLQL<sup>26</sup> and after addition of streptavidin-phycoerythrin (PE) (BD Biosciences). Labeling of HUVEC, Jurkat and Jurkat-CD160 by PE-conjugated HLA-G tetramers was performed at 37°C for 1 hour. For Jurkat-CD160 and Jurkat, tetramers were cross-linked with anti-HLA class I W6/32 mAb, as previously described.<sup>27</sup>

### **In vitro capillary tube formation assay**

Growth factor reduced Matrigel (BD Biosciences,) was diluted in collagen (1/6 v/v) and kept on ice. 160 µL of this solution was added to each well of 8-well culture slides precoated with type I rat tail collagen and left at 37°C for 1 hour. A HUVEC suspension, untreated or treated with FGF2 (10 ng/mL), sHLA-G1 (1 µg/mL), sHLA-G1mono (1 µg/mL), mAb CD160 (1 or 10 µg/mL) or IgG1 isotype control (10 µg/mL) was seeded into the Matrigel/collagen gel for 24 hours at 37°C. Microtubules were quantified by microscopy as previously described.<sup>28</sup> Briefly, the culture medium was removed, cells rinsed twice with PBS and fixed for 30 minutes at room temperature in a 4% paraformaldehyde solution. Then, the cells were washed twice with PBS and stained with Masson's Trichrome. The extent of the microcapillary network was measured using an automated computer-assisted image analysis system (Imagenia Biocom, Courtaboeuf, France), and the total length of the capillaries in each well was determined. The mean microcapillary network length (µm) was calculated for each experimental condition. Experiments were performed in triplicate and repeated 3 times.

### **Apoptosis assays**

Apoptosis was evaluated by two methods: time-lapse microscopy<sup>29</sup> and flow cytometry analysis using the FITC-conjugated Annexin V/PI assay.<sup>30</sup> For the time-lapse microscopy assay, HUVEC, SGHEC-7 endothelial or SGHPL-4 trophoblast cell lines were seeded into 6-well plates at  $2.5 \times 10^5$  cells/well in normal culture medium as described earlier.<sup>21,22</sup> After 15 hours, sHLA-G1, sHLA-G1mono (0.1 or 1  $\mu\text{g/mL}$ ), CL1-R2 anti-CD160 mAb (1-10  $\mu\text{g/ml}$ ), IgG1 isotype control (10  $\mu\text{g/mL}$ ) or zVAD-fmk (50  $\mu\text{mol/l}$ , Calbiochem) were added to the wells. The plate was transferred to an Olympus IX70 inverted fluorescence microscope with motorized stage and cooled CCD camera and enclosed in a heated, humidified chamber at 37°C in 5% CO<sub>2</sub>. Images were taken every 15 minutes for 0-50 hours and time-lapse sequences were analyzed using ImagePro Plus (Media Cybernetics). In each field of view 40 cells were randomly chosen. The experiments were repeated at least four times. Apoptotic cells were scored according to the time at which clear apoptotic morphology was first observed.<sup>29</sup> For the Annexin-V/PI assay,  $2 \times 10^5$  cells were seeded into a 6-well plate in RPMI 1% FCS for 24 hours and then incubated for an additional 12 hours in RPMI 0.5% FCS. Cells were treated or not with sHLA-G1 (1  $\mu\text{g/mL}$ ), mAb CD160 (10  $\mu\text{g/mL}$ ) or control IgG1 (10  $\mu\text{g/mL}$ ) for 50 hours in the presence of VEGF (50 ng/mL). At the end of the treatment, the floating cells were collected by centrifugation, whereas adherent cells were harvested by trypsin-EDTA solution to produce a single cell suspension. The cells were then pelleted by centrifugation and washed twice with PBS. Apoptotic cell death was identified by double staining with FITC-conjugated Annexin-V and PI, using the Annexin V-FITC Apoptosis Detection kit (DAKO) according to manufacturer's instructions. Cells were analyzed by flow cytometry on a FACScan (Becton Dickinson) using the fluorescence 1 (FL1-540 nm) signal detector for FITC conjugates and the fluorescence 2 (FL2-600 nm) signal detector for PI. Ten thousand events were recorded for each sample. The data were analyzed using CellQuest software.

### **Western blot analysis of cleaved PARP expression**

SGHEC-7 endothelial cells were seeded in culture plates. After 16 hours the cells were incubated with sHLA-G1 (0.1  $\mu\text{g/mL}$ ) for 60 hours. Cells were lysed in RIPA buffer with 0.1 mg/mL PMSF, 30  $\mu\text{l/mL}$  aprotinin (Sigma A6279 solution at 5-10 trypsin inhibitor units/mL), and 1 mmol/L sodium orthovanadate at 4°C for 30 minutes. Equal

amounts of proteins determined by Bradford assay were loaded and separated by SDS-PAGE and transferred to a nitrocellulose membrane. Following incubation in blocking buffer for 1 hour at room temperature, the membrane was incubated with rabbit polyclonal anti-human cleaved PARP (Promega, Southampton, UK) for 1 hour. Anti-rabbit IgG peroxidase (A6154, Sigma) was added for 1 hour. Detection of membrane bound mAb was carried out by chemiluminescence (ECLPlus, Amersham). Actin expression after stripping and reprobing the blot confirmed equal loading.

### **Rabbit Corneal Angiogenesis Assay**

The corneal pocket assay used in this study has been previously described.<sup>31</sup> Male New Zealand albino rabbits were anaesthetized. A corneal pocket was created by incision on the superior side of the corneal stroma 2 mm away from the limbus. Slow releasing implants of hydrogel hydrated with PBS containing FGF2 (500 ng) were inserted into this pocket. 24 and 72 hours after the pellet implantation, 5  $\mu$ g of sHLA-G1 (1 mg/mL in PBS) or an equal volume of PBS (control) were injected into the subconjunctiva on the superior side near the limbus. Neovascularization of the cornea was measured on day 8 after implantation by microscopic examination with a slit lamp and scored according to a five-grade scale (grade 0, normal avascular cornea; grade 1, <1 mm long neovessels; grade 2, 1 mm long neovessels; grade 3, 1-2 mm long neovessels; grade 4, neovessels extending to the implant). The average mean score obtained after implantation of a pellet containing no angiogenic factor is < 0.5.<sup>31</sup> Means and standard deviations were determined on eight implant per group.

### **VEGF and sHLA-G1 cell binding competition experiments**

VEGF and sHLA-G1 were radiolabeled with Na<sup>125</sup>I to a specific activity of  $2.4 \times 10^4$  and  $1.1 \times 10^5$  cpm/ng, respectively.<sup>32</sup> Wells containing  $2 \times 10^5$  serum-starved HUVEC were either untreated or pre-treated with of VEGF (0.1  $\mu$ g/mL) or FGF2 (0.1  $\mu$ g/mL) or sHLA-G1 (0.1, 1.0 or 10  $\mu$ g/mL) at 37°C for 24 hours or processed immediately for binding assays. Briefly, dishes were rinsed in cold DMEM supplemented with 0.2% gelatin and 20 mM HEPES (pH 7.3) and incubated at 4°C for 2 hours with 2 ng/mL <sup>125</sup>I-VEGF or <sup>125</sup>I-sHLA-G1 in the absence or presence of indicated concentrations of cold competitors. Cells were then rinsed in the same medium, lysed in 0.02M Tris, 10 mM

EDTA, 0.3M NaCl, 0.1% SDS, 1% Triton X-100, 0.05% Tween 20 RIPA buffer and radioactivity counted in a  $\gamma$  counter.

### **Cell phenotyping**

Subconfluent HUVEC, HVMEC, HAOSMC or fibroblasts were scraped in PBS-EDTA and incubated in the presence or absence of 0.1  $\mu\text{g}/\text{mL}$  of sHLA-G1 at 4°C. After 2 hours, cells were incubated with anti-CD8, -CD85d, -CD85j, or CL1-R2 anti-CD160 specific mAbs or Ig-isotype control (20  $\mu\text{g}/\text{mL}$ ) followed by F(ab')<sub>2</sub>-FITC or -PE-conjugated anti-mouse IgG. Non-viable cells were excluded by the use of propidium iodide (PI). Samples were analyzed on a Coulter-Epics ELITE flow cytometer.

### **Reverse transcription-polymerase chain reaction, and cDNA sequencing**

CD160 transcripts were detected by RT-PCR using the following primer sequences: 5'-TGCAGGATGCTGTTGGAACCC-3' and 3'-TCAGCCTGAACTGAGAGTGCCTTC-5'. cDNA quality was confirmed by amplification of  $\beta$ -actin using the appropriate primers. Amplification conditions for CD160 and  $\beta$ -actin were 95°C for 45 seconds, 60°C for 30 seconds, and 72°C for 1 minute (35 cycles), using a MJ Research PTC-200 Peltier Thermal Cycler (Biorad, Marnes-la-Coquette, France). For the CD160 sequencing, a Taq High Fidelity was used (Invitrogen). PCR product was purified (qiaex II, Qiagen) and analyzed with the following primer sequences:

BY01 (5'-TGCAGGATGCTGTTGGAACCC-3'),

BY03 (3'-TCAGCCTGAACTGAGAGTGCCTTC-5'),

BY02 (5'CAGCTGAGACTTAAAAGGGATC-3') and

BY04 (3'-CACCAACACCATCTATCCCAG-5').

### **Immunohistochemistry**

Sub-confluent Lewis lung carcinoma cells were trypsinized, washed twice and suspended in PBS.  $2 \times 10^5$  cells were injected subcutaneously into the dorsal midback region of C57BL/6 female mice (Iffa-Credo, L'Arbresle, France). Tumors were taken on day 21, fixed with 10% formalin (Sigma) overnight at 4°C, and embedded in paraffin (Embeder Leica). 5  $\mu\text{m}$  sections were placed in a Dako Autostainer and incubated with TNB blocking buffer (TSA kit, NEN), peroxidase-blocking reagent (DAKO) and mouse immunoglobulin blocking reagent (Vector Laboratories, Paris, France). Sections were incubated with CL1-R2 anti-CD160 mAb (10  $\mu\text{g}/\text{mL}$ ), followed by biotin-labeled goat

anti-mouse IgG and avidin-biotin complex (Vector Laboratories). They were stained with DAB (Vector Laboratories), counterstained with hematoxylin, viewed on a Nikon microscope (E-800) and digitized using a DMX 1200 camera (Nikon) with 40 x objective.

### **Statistical analysis**

Where applicable, results are presented as mean  $\pm$  SEM or SD of "n" independent experiments and assessed using the Mann Whitney *U*, ANOVA or Student *t* tests as appropriate and Everstat or GraphPadPrism software with  $P < 0.05$  considered significant.

## **Results**

### **sHLA-G1 inhibits FGF2-mediated capillary tube formation**

We investigated whether sHLA-G1 heavy chain non covalently associated with  $\beta 2m$  could interfere with pro-angiogenic factor functions *in vitro*. We evaluated the capacity of sHLA-G1 to inhibit capillary tube formation by endothelial cells cultured on Matrigel. Purified recombinant sHLA-G1, when added exogenously to HUVEC, significantly inhibited FGF2-induced tubule-like formation (Figures 1A, morphology and 1B, quantification). In contrast, the sHLA-G1<sub>mono</sub> negative control had no effect. These findings indicate that sHLA-G1 inhibits *in vitro* pro-angiogenic factor-mediated endothelial cell capillary tube formation.

### **sHLA-G1 induces apoptosis of endothelial cells**

Having shown the inhibitory effect of sHLA-G1 on a function that is relevant to angiogenesis (tubule formation), we then used apoptosis assays to interrogate the possible mechanisms by which sHLA-G1 was altering the end point of angiogenesis. Apoptosis is indeed an important regulator of angiogenesis.<sup>33</sup> We found that incubation of HUVEC with recombinant sHLA-G1 clearly induced apoptosis, as determined by time-lapse digital image microscopy (Figure 2). Phase contrast images of the experiment (Figure 2A) and video data (Movies 1 and 2) show that sHLA-G1-treated cell morphology was characterized by cytoplasmic and nuclear shrinkage and by a change to a phase bright appearance, as well as the formation of membrane blebs/blisters (Figure 2A). Such effect of sHLA-G1, but not of sHLA-G1<sub>mono</sub>, was

time-dependent (Figure 2B). Comparable kinetics curve was obtained using SGHEC-7 cells (data not shown). Similar apoptotic effects of sHLA-G1 were observed on HUVEC by using Annexin V/PI assay (Figure 6D). The endothelial cell type specificity of this sHLA-G1-induced apoptosis was demonstrated by the absence of any significant effect of this molecule on human trophoblast cells (Figure 2C) or fibroblasts in primary culture (Figure 6D). Use of the broad-spectrum caspase inhibitor zVAD-fmk prevented recombinant sHLA-G1-mediated apoptosis (Figure 2D), implicating the caspase pathway in the sHLA-G1-mediated apoptosis of endothelial cells. This was further demonstrated by the detection of cleaved poly (ADP-ribose) polymerase (PARP) by Western blot analysis after sHLA-G1 treatment of endothelial cells (Figure 2E). By contrast, no p85 cleaved PARP was detected after a similar sHLA-G1 treatment of trophoblast cells (Supplementary Figure 2). These findings together demonstrate that sHLA-G1 induces caspase-dependent apoptosis of endothelial cells.

#### **sHLA-G1 inhibits corneal angiogenesis *in vivo*.**

A rabbit corneal pocket assay was used to determine whether sHLA-G1 could also inhibit angiogenesis *in vivo*. Neovascularization arised from the limbus toward the FGF2-containing pellet and was easily detected after 8 days in the control corneas (Figure 3A, left hand-side photograph). In contrast, the injection of sHLA-G1 (Figure 3A, right hand-side photograph) almost totally abrogated the corneal neovascularization. These results reproduced on 8 implant per group (Figure 3B) clearly demonstrate that sHLA-G1 has an anti-angiogenic effect on FGF2-induced angiogenesis *in vivo*.

#### **sHLA-G1 binds directly to the CD160 receptor**

It was then important to identify the receptor involved in the anti-angiogenic effects of sHLA-G1. We first tested whether sHLA-G1 interfered with VEGF receptors, by performing radioreceptor-assay binding experiments at 4°C on HUVEC incubated for 2 hours (equilibrium time) with <sup>125</sup>I-VEGF or <sup>125</sup>I-sHLA-G1 in the presence of various concentrations of cold competitors. We first analyzed the binding of <sup>125</sup>I-sHLA-G1 to HUVEC and found that cold VEGF or FGF2 competitors had no effect, whereas unlabeled sHLA-G1 inhibited this binding as a function of concentration, with IC50 values in the nanomolar range (Figure 4A). In competition experiments using <sup>125</sup>I-VEGF as ligand, we found that cold VEGF displaced its binding to HUVEC with IC50

values in the nanomolar range, whereas sHLA-G1 had no effect (Figure 4B). Furthermore, we found that cold sHLA-G1 competitor did not inhibit the binding of  $^{125}\text{I}$ -VEGF to porcine aortic endothelial cells (PAEC)-VEGF-R2 or PAEC-NPL1 transfectants (data not shown). These results demonstrate that sHLA-G1 bound specifically to endothelial cells without interfering with the VEGF receptors.

Using flow cytometry and specific mAbs, we investigated whether HUVEC expressed some of the HLA-G receptors described to date, including CD8,<sup>6</sup> ILT4/CD85d,<sup>34</sup> ILT2/CD85j,<sup>34</sup> and CD160.<sup>27</sup> We found that HUVEC expressed CD160, although not with constant levels, but not CD8, CD85d or CD85j (Figure 5A). Similarly, HMVEC also bound anti-CD160 mAb (Figure 5A), as did bovine endothelial cells (data not shown), suggesting that the CD160 epitope recognized by this mAb was conserved among species. In contrast, smooth muscle cells and fibroblasts in primary culture did not express CD160 (Figure 5A). To confirm that CD160 is expressed by HUVEC, we performed RT-PCR analysis, using CD160 specific primers. We demonstrated that the CD160 mRNA was present in HUVEC, similarly to the NK92 cell line, whereas CD4<sup>+</sup> T cells were negative (Figure 5B). It should be noted that HUVEC did not express the potential HLA-G receptor KIR2DL4 transcripts (data not shown). Then HUVEC and NK92 cDNAs were isolated and sequenced. Predicted amino acid sequence alignment of HUVEC and NK92 CD160 proteins showed that they were both similar to the CD160 sequence already published,<sup>20</sup> with the exception of two substituted residues (Figure 5C), indicating a possible allelic form.

We then investigated whether CD160 was also expressed on endothelial cells *in vivo* and did not result from culture conditions. For this purpose, Lewis lung carcinoma cells were injected subcutaneously in C57/BL6 mice. Immunohistochemical analysis of the tumor was performed at day 21, using the CL1-R2 anti-CD160 mAb. We found that this mAb strongly stained endothelial cells of microvessels at the periphery of the tumors (Figures 6A and 6B) and inside them (Figures 6C and 6D), whereas no staining was detected with IgG isotype control (data not shown). In contrast, tumor cells remained unstained. Such reactivity of this anti-human CD160 mAb is not surprising as the previous identification and sequencing of both human and mouse CD160 encoding cDNA revealed a strong homology between the two species.<sup>20,35</sup> We then analyzed whether sHLA-G1 could effectively bind to the CD160 receptor expressed by endothelial cells. We first found that a HLA-G1 tetramer specifically bound to HUVEC like it did on CD160-transfected Jurkat but not on parental Jurkat cells (Figure 7A).

sHLA-G1-CD160 direct interaction on HUVEC was further demonstrated by showing that pre-incubation of HUVEC with recombinant sHLA-G1 specifically blocks the binding of anti-CD160 mAb (Figure 7B), whereas a pre-incubation with VEGF did not (data not shown).

To further demonstrate that sHLA-G1 anti-angiogenic function is mediated through interaction with CD160, we tested whether soluble anti-CD160 mAb could antagonize or mimic the sHLA-G1 activity in the *in vitro* Matrigel tube and apoptosis assays. The results clearly showed that CL1-R2 mAb mimicked sHLA-G1 as it inhibited FGF2-mediated tubule vessel growth (Figure 7C) and induced HUVEC apoptosis, as demonstrated by Annexin V/PI assay (Figure 7D) and time-lapse microscopy (data not shown). CD160 mAb-mediated apoptosis of HUVEC is similar to the sHLA-G1-mediated apoptosis, whereas none of these apoptosis inducers are active on control fibroblast cells in primary culture (Figure 7D). Altogether, these data further demonstrate that CD160 expressed by endothelial cells is a functional receptor able to trigger an anti-angiogenic cell response.

## Discussion

In this study, we demonstrated that the sHLA-G1 molecule, known to exert immune regulatory functions,<sup>1</sup> also displays anti-angiogenic properties both *in vitro* and *in vivo*. This includes inhibition of vessel formation, induction of endothelial cell apoptosis and *in vivo* inhibition of FGF2-induced rabbit corneal neoangiogenesis. Spatial and temporal regulation of the vasculature at the maternal-fetal interface plays an important role in ensuring adequate blood supply to nourish the developing embryo, suggesting that there are locally acting factors that regulate vascular cells.<sup>36</sup> The ability of sHLA-G1 to induce apoptosis of both confluent and proliferating endothelial cells might be relevant in the utero-placental environment, since effacement of preexisting maternal endothelial cells rather than inhibition of angiogenesis would be required. Soluble HLA-G1 is indeed secreted by endovascular trophoblast that replace vascular cells of the maternal spiral arteries, thereby increasing the diameter of these vessels several fold and transforming them into high conductance vessels.<sup>12</sup> We hypothesize that during early pregnancy, sHLA-G1 apoptotic effects on these maternal endothelial cells might contribute to such replacement and vascular remodeling. Defects of HLA-G expression, including

diminishment of soluble HLA-G in preeclamptic placentas, characterized by a shallow cytotrophoblast invasion and a reduced flow of maternal blood to the fetoplacental unit,<sup>37</sup> favors such a hypothesis. A recent report using an *ex vivo* model of maternal spiral artery perfused with extravillous cytotrophoblast, has shown that addition of these cells induced apoptosis of endothelial cells.<sup>38</sup> Knowing that extravillous cytotrophoblast do produce sHLA-G,<sup>4</sup> one can think that such apoptosis is mediated by sHLA-G.

Different mechanisms have been reported to explain the activity of angiogenesis inhibitors, including inhibition of endothelial cell remodeling,<sup>39</sup> induction of endothelial cell apoptosis,<sup>40</sup> or chemorepulsion of endothelial cells.<sup>41</sup> In this report we demonstrate novel inhibitory actions of sHLA-G1 directed to endothelial cells. In addition, we report that sHLA-G1-treated endothelial cells progressively showed apoptotic morphology. The mechanism of this induced apoptosis remains incompletely characterized despite clear implication of caspases (Figures 2D and 2E). The Fas/FasL pathway might also be involved as it has been shown for the sHLA-G1-induced apoptosis of activated CD8<sup>+</sup> T cells.<sup>6</sup> It is interesting that a role for apoptosis and Fas/FasL interactions in the remodeling of uterine arteries during pregnancy has recently been demonstrated.<sup>38</sup>

In this study, we also used the sHLA-G1- $\beta$ 2m fusion monochain (sHLA-G1<sub>mono</sub>)<sup>23</sup> as a negative control molecule prepared and purified exactly like the conformational sHLA-G1. This control molecule did not exhibit anti-angiogenic activities in the assays described in this report. It is unlikely that the conformation of this construct was grossly altered since the W6/32 conformational mAb still recognized it (see Materials & Methods). However, it is possible that the presence of a  $\beta$ 2m-linked 15-residue spacer to sHLA-G1 heavy chain impairs the formation of sHLA-G1<sub>mono</sub> multimers. As it has been shown that the oligomerization of sHLA-G1 is essential for its activity and efficient recognition by CD85j/ILT2 receptors,<sup>42</sup> this might explain the unresponsiveness of sHLA-G1<sub>mono</sub> which might not bind to CD160 for the same reason. This hypothesis is supported by the recently published crystal structure of the HLA-G protein presenting a model of HLA-G oligomers and the relative position of the CD85j/ILT2 receptor near the complex.<sup>43</sup> It has also been shown that HLA-G can be found as a free heavy chain due to the dissociation of  $\beta$ 2m from the conformed protein.<sup>44</sup> Moreover,  $\beta$ 2m-free HLA-G and conformed HLA-G can form complexes able to modulate HLA-G affinity to some NK receptors.<sup>44</sup> In the sHLA-G1<sub>mono</sub> construct the  $\beta$ 2m is covalently linked to the HLA-G1 heavy chain, such a mechanism of dissociation

of the  $\beta 2m$  from the heavy chain would thus be impossible and this might contribute to the inefficiency of sHLA-G1<sub>mono</sub> to activate CD160 present on endothelial cells.

The direct inhibitory effect of sHLA-G1 on vessel formation is most likely mediated through the functional CD160 receptor, as the CL1-R2 anti-CD160 mAb mimics the inhibition of FGF2-induced capillary tubule formation by endothelial cells cultured in Matrigel as well as the induction of endothelial cell apoptosis. sHLA-G1 acts directly on CD160 receptor. Knowing that various HLA class I molecules may bind to CD160,<sup>27</sup> it cannot be excluded that other soluble MHC class I molecules could also trigger this receptor to exert anti-angiogenic functions. Collectively these findings provide important mechanistic insights into anti-angiogenic action of sHLA-G1. Further investigation is needed to determine and compare the signaling pathways used by endothelial cells and NK cells following CD160 engagement and leading to anti-angiogenic activities and endothelial cell apoptosis for the former and cytokine production<sup>45</sup> and cytotoxicity<sup>23</sup> for the latter.

In addition to the clear importance in the placental/uterine environment, the identification of CD160 as an inhibitory signaling receptor for angiogenesis could be useful for experimental anti-angiogenic therapy to prevent tumor cell growth. Our immunohistochemical analysis of a mouse grafted tumor showed that CD160, encoded by a gene conserved in this species,<sup>35,46</sup> was present in endothelial cells of the tumor vasculature but was not expressed by tumor cells. Future goals are therefore to examine the potential CD160/sHLA-G1 mediated anti-angiogenic effect in different tumors and explore the possible therapeutic use of CD160 mAb in the regulation of pathological neovascularization.

## Acknowledgments

We thank D<sup>r</sup> Marco Colonna for the gift of CD85d mAb, D<sup>r</sup> Dan Geraghty for the gift of 721.221-sHLA-G1 cells, and P<sup>r</sup> Alain Hovnanian for the gift of primary fibroblasts. Isabelle Senegas, Josette Desjobert, Carine Berge, and Marie-Claude Laplace are gratefully acknowledged for their contribution to this work.

## References

1. Le Bouteiller P, Blaschitz A. The functionality of HLA-G is emerging. *Immunol Rev.* 1999;167:233-244.
2. Fujii T, Ishitani A, Geraghty DE. A soluble form of the HLA-G antigen is encoded by a messenger ribonucleic acid containing intron 4. *J Immunol.* 1994;153:5516-5524.

3. Dong Y, Lieskovska J, Kedrin D, Porcelli S, Mandelboim O, Bushkin Y. Soluble nonclassical HLA generated by the metalloproteinase pathway. *Hum Immunol.* 2003;64:802-810.
4. Morales P, Pace J, Platt J, et al. Placental cell expression of HLA-G2 isoforms is limited to the invasive trophoblast phenotype. *J Immunol.* 2003;171:6215-6224.
5. Contini P, Ghio M, Poggi A, et al. Soluble HLA-A,-B,-C and -G molecules induce apoptosis in T and NK CD8<sup>+</sup> cells and inhibit cytotoxic T cell activity through CD8 ligation. *Eur J Immunol.* 2003;33:125-134.
6. Fournel S, Aguerre-Girr M, Huc X, et al. Cutting Edge: Soluble HLA-G1 triggers CD95/CD95 ligand-mediated apoptosis in activated CD8<sup>+</sup> cells by interacting with CD8. *J Immunol.* 2000;164:6100-6104.
7. Lila N, Rouas-Freiss N, Dausset J, Carpentier A, Carosella ED. Soluble HLA-G protein secreted by allo-specific CD4<sup>+</sup> T cells suppresses the allo-proliferative response: a CD4<sup>+</sup> T cell regulatory mechanism. *Proc Natl Acad Sci USA.* 2001;98:12150-12155.
8. Blaschitz A, Lenfant F, Mallet V, et al. Endothelial cells in chorionic fetal vessels of first trimester placenta express HLA-G. *Eur J Immunol.* 1997;27:3380-3388.
9. Dye JF, Jablenska R, Donnelly JL, et al. Phenotype of the Endothelium in the Human Term Placenta. *Placenta.* 2001;22:32-43.
10. Lim KH, Zhou Y, Janatpour M, et al. Human cytotrophoblast differentiation/invasion is abnormal in pre-eclampsia. *Am J Pathol.* 1997;151:1809-1818.
11. Yie SM, Li LH, Li YM, Librach C. HLA-G protein concentrations in maternal serum and placental tissue are decreased in preeclampsia. *Am J Obstet Gynecol.* 2004;191:525-529.
12. Moffett-King A. Natural killer cells and pregnancy. *Nat Rev Immunol.* 2002;2:656-663.
13. Dorling A, Monk N, Lechler R. HLA-G inhibits the transendothelial migration of human NK cells. *Eur J Immunol.* 2000;30:586-593.
14. Forte P, Pazmany L, Matter-Reissmann UB, Stussi G, Schneider MK, Seebach JD. HLA-G Inhibits Rolling Adhesion of Activated Human NK Cells on Porcine Endothelial Cells. *J Immunol.* 2001;167:6002-6008.
15. Folkman J. Angiogenesis in cancer, vascular, rheumatoid and other disease. *Nat Med.* 1995;1:27-31.
16. Ferrara N, Gerber HP, LeCouter J. The biology of VEGF and its receptors. *Nat Med.* 2003;9:669-676.
17. Carmeliet P. Angiogenesis in life, disease and medicine. *Nature.* 2005;438:932-936.
18. Ferrara N, Kerbel RS. Angiogenesis as a therapeutic target. *Nature.* 2005;438:967-974.
19. Maiza H, Leca G, Mansur IG, Schiavon V, Boumsell L, Bensussan A. A novel 80-kD cell surface structure identifies human circulating lymphocytes with natural killer activity. *J Exp Med.* 1993;178:1121-1126.
20. Anumantha A, Bensussan A, Boumsell L, et al. Cloning of BY55, a novel Ig superfamily member expressed on NK cells, CTL, and intestinal intraepithelial lymphocytes. *J Immunol.* 1998;161:2780-2790.
21. Cartwright JE, Holden DP, Whitley GS. Hepatocyte growth factor regulates human trophoblast motility and invasion: a role for nitric oxide. *Br J Pharmacol.* 1999;128:181-189.
22. Fickling SA, Tooze JA, Whitley GS. Characterization of human umbilical vein endothelial cell lines produced by transfection with the early region of SV40. *Exp Cell Res.* 1992;201:517-521.
23. Le Bouteiller P, Barakonyi A, Giustiniani J, et al. Engagement of CD160 receptor by HLA-C is a triggering mechanism used by circulating natural killer (NK) cells to mediate cytotoxicity. *Proc Natl Acad Sci USA.* 2002;99:16963-16968.
24. Fournel S, Aguerre-Girr M, Campan A, et al. Soluble HLA-G: purification from eucaryotic transfected cells and detection by a specific ELISA. *Am J Reprod Immunol.* 1999;42:22-29.
25. Allan DS, Colonna M, Lanier LL, et al. Tetrameric complexes of human histocompatibility leukocyte antigen (HLA)-G bind to peripheral blood myelomonocytic cells. *J Exp Med.* 1999;189:1149-1156.
26. Lee N, Malacko AR, Ishitani A, et al. The membrane-bound and soluble forms of HLA-G bind identical sets of endogenous peptides but differ with respect to TAP association. *Immunity.* 1995;3:591-600.
27. Agrawal S, Marquet J, Freeman GJ, et al. Cutting edge: MHC class I triggering by a novel cell surface ligand costimulates proliferation of activated human T cells. *J Immunol.* 1999;162:1223-1226.
28. Ruggeri B, Singh J, Gingrich D, et al. CEP-7055: a novel, orally active pan inhibitor of vascular endothelial growth factor receptor tyrosine kinases with potent antiangiogenic activity and antitumor efficacy in preclinical models. *Cancer Res.* 2003;63:5978-5991.
29. Dash PR, Cartwright JE, Baker PN, Johnstone AP, Whitley GS. Nitric oxide protects human extravillous trophoblast cells from apoptosis by a cyclic GMP-dependent mechanism and independently of caspase 3 nitrosylation. *Exp Cell Res.* 2003;287:314-324.

30. Vermes I, Haanen C, Steffens-Nakken H, Reutelingsperger C. A novel assay for apoptosis. Flow cytometric detection of phosphatidylserine expression on early apoptotic cells using fluorescein labelled Annexin V. *J Immunol Methods*. 1995;184:39-51.
31. Binetruy-Tournaire R, Demangel C, Malavaud B, et al. Identification of a peptide blocking vascular endothelial growth factor (VEGF)-mediated angiogenesis. *Embo J*. 2000;19:1525-1533.
32. Plouët J, Moro F, Bertagnolli S, et al. Extracellular cleavage of the vascular endothelial growth factor 189-amino acid form by urokinase is required for its mitogenic effect. *J Biol Chem*. 1997;272:13390-13396.
33. Jain RK. Molecular regulation of vessel maturation. *Nat Med*. 2003;9:685-693.
34. Shiroishi M, Tsumoto K, Amano K, et al. Human inhibitory receptors Ig-like transcript 2 (ILT2) and ILT4 compete with CD8 for MHC class I binding and bind preferentially to HLA-G. *Proc Natl Acad Sci USA*. 2003;100:8856-8861.
35. Maeda M, Carpetino C, Russell R, et al. Murine CD160, Ig-like receptor on NK cells and NKT cells, recognizes classical and non classical MHC class I and regulates NK cell activation. *J Immunol*. 2005;175:4426-4432.
36. Ong S, Lash G, Baker PN. Angiogenesis and placental growth in normal and compromised pregnancies. *Baillieres Best Pract Res Clin Obstet Gynaecol*. 2000;14:969-980.
37. Redman CW, Sargent IL. Latest advances in understanding preeclampsia. *Science*. 2005;308:1592-1594.
38. Ashton SV, Whitley GS, Dash PR, et al. Uterine spiral artery remodeling involves endothelial apoptosis induced by extravillous trophoblasts through Fas/FasL interactions. *Arterioscler Thromb Vasc Biol*. 2005;25:102-108.
39. Serini G, Valdembri D, Zanivan S, et al. Class 3 semaphorins control vascular morphogenesis by inhibiting integrin function. *Nature*. 2003;424:391-397.
40. Folkman J. Angiogenesis and apoptosis. *Semin Cancer Biol*. 2003;13:159-167.
41. Bielenberg DR, Hida Y, Shimizu A, et al. Semaphorin 3F, a chemorepellant for endothelial cells, induces a poorly vascularized, encapsulated, nonmetastatic tumor phenotype. *J Clin Invest*. 2004;114:1260-1271.
42. Gonen-Gross T, Achdout H, Gazit R, et al. Complexes of HLA-G protein on the cell surface are important for leukocyte Ig-like receptor-1 function. *J Immunol*. 2003;171:1343-1351.
43. Clements CS, Kjer-Nielsen L, Kostenko L, et al. Crystal structure of HLA-G: a nonclassical MHC class I molecule expressed at the fetal-maternal interface. *Proc Natl Acad Sci USA*. 2005;102:3360-3365.
44. Gonen-Gross T, Achdout H, Arnon TI, et al. The CD85J/Leukocyte Inhibitory Receptor-1 Distinguishes between Conformed and  $\beta$ 2-Microglobulin-Free HLA-G Molecules. *J Immunol*. 2005;175:4866-4874.
45. Barakonyi A, Rabot M, Marie-Cardine A, et al. Cutting edge: engagement of CD160 by its HLA-C physiological ligand triggers a unique cytokine profile secretion in the cytotoxic peripheral blood NK cell subset. *J Immunol*. 2004;173:5349-5354.
46. Bensussan A. BY55 (CD160). *PROW*. 2000;1:72-73.

## Figure Legends

**Figure 1. sHLA-G1 inhibits FGF2-mediated HUVEC capillary tubule-like formation.** (A) In vitro tubule-like capacity of HUVEC. HUVEC were seeded on Matrigel in the absence (UT, untreated) or presence of FGF2 (10 ng/mL) and after addition of sG1 or sG1<sub>mono</sub> (1 µg/mL). Photographs of each well were taken after 24 hours, and angiogenesis was quantified as described in Materials and Methods. This Figure is representative of 5 separated experiments each performed in triplicate. After sG1 treatment, the branches and tubules formed were much less developed compared to sG1<sub>mono</sub>-treated or untreated HUVEC. (B) Branches from each cell were counted from 1 representative field per well. Data indicate mean of 3 wells +/- SEM of triplicates and are representative of 5 independent experiments. \*\*\* $P < 0.001$ , ANOVA test.

**Figure 2. sHLA-G1 induces apoptosis of endothelial cells.** (A) Time-lapse digital image microscopy of HUVEC after treatment with sHLA-G1. Apoptotic morphology could be detected over time, evidenced by cytoplasmic retraction and a phase-bright appearance and membrane blebbing and blistering. These apoptotic changes are also illustrated in Supplementary video clip online. (B) Kinetics curve of apoptosis induction. HUVEC were untreated (control) or incubated with sHLA-G1 (sG1, 1 µg/mL) or sHLA-G1<sub>mono</sub> (sG1 mono, 1 µg/mL). Time-lapse microscopy was carried out to assess the appearance of apoptotic morphology. Although data were obtained every 15 minutes, data points are only shown every 2 hours for clarity. Mean ± SEM of pooled data from 4 experiments is shown.  $P < 0.001$  between sHLA-G1 and sHLA-G1<sub>mono</sub> or control at 50 hours time-point, repeated measures ANOVA with Tukey's post test. (C) Kinetics curve of apoptosis induction of trophoblast cells after incubation with sHLA-G1, compared to untreated (control) cells. Mean ± SEM of pooled data from 4 experiments is shown. Non-significant between sHLA-G1 and control at 50 hours time-point, Mann Whitney  $U$  test ( $p$  value: 0.1143) or paired  $t$  test ( $p$  value: 0.1265). (D) SGHEC-7 endothelial cell apoptosis induction by sG1 (0.1 µg/mL), compared to untreated (control) cells, in the presence or absence of the caspase inhibitor zVAD-fmk assessed by time-lapse microscopy. Mean ± SEM of pooled data from 4 experiments is shown. The area under the curve was calculated from the kinetics curves. \*\*\* $P < 0.001$  ANOVA test. (E) Western blot analysis of p85 cleaved PARP expression. SGHEC-7

endothelial cells were incubated in the absence (control) or presence of sG1 (0.1  $\mu\text{g}/\text{mL}$ ) for 60 hours (confluent monolayer).

**Figure 3. sHLA-G1 inhibits FGF2-induced corneal angiogenesis *in vivo*.** The neovascularization was assessed 8 days after insertion of implants containing FGF2 in rabbit corneal pockets, in the presence or absence of sHLA-G1 (5  $\mu\text{g}/\text{injection}$ ). (A) A representative photograph of each group (control, PBS subconjunctival injections; sG1, sHLA-G1 subconjunctival injections) at day 8 after FGF2 pellet implantation. Arrows = pellet implants; Arrowhead indicates the newly formed vessels. Magnification,  $\times 16$ . (B) Neovascularization (NV) scores  $\pm$  SEM for 8 implant groups.  $*P < 0.001$ , Student t test.

**Figure 4. sHLA-G1 does not interfere with VEGF receptors.** (A) HUVEC were incubated with  $^{125}\text{I}$ -sHLA-G1 (2  $\text{ng}/\text{mL}$ , ie 50 pM) in the absence (-) or presence of cold VEGF (1  $\mu\text{g}/\text{mL}$ ), FGF2 (1  $\mu\text{g}/\text{mL}$ ) or sHLA-G1 (sG1, 0.1, 1.0 or 10  $\mu\text{g}/\text{mL}$ ). Unlabeled sG1 but not VEGF or FGF2 prevented  $^{125}\text{I}$ -sHLA-G1 binding. (B) HUVEC were incubated with  $^{125}\text{I}$ -VEGF (2  $\text{ng}/\text{mL}$ ) in the presence of cold sG1, FGF2 or VEGF. Unlike cold VEGF, cold sG1 did not abrogate iodinated VEGF binding. In these conditions, the IC<sub>50</sub> of cold ligands were 200 pM for VEGF and 2500 pM for sHLA-G1. Results are means  $\pm$  SEM of triplicate wells and are representative of 3 independent experiments.

**Figure 5. Both HUVEC and HMVEC express the CD160 receptor.** (A) HUVEC, HMVEC, HAOSMC and fibroblasts in primary culture were analyzed by flow cytometry after incubation with either anti-CD8, -CD85d, -CD85j or CL1-R2 (anti-CD160) specific mAbs (open profiles) or IgG isotype controls (black profiles) followed by PE-labeled conjugates. Results are representative of 6 independent experiments. (B) CD160 mRNA was expressed by HUVEC and NK92 cells (positive control) but not CD4<sup>+</sup> T cells (negative control): RT-PCR analysis, using CD160 specific primers, compared with  $\beta$ -actin control primers. (C) Predicted amino acid sequence alignment of CD160 expressed in HUVEC and NK92. (–) indicates identity.

**Figure 6. Immunohistochemical staining of Lewis lung carcinoma tumor sections with anti-CD160 mAb demonstrating CD160 positive vessels.** (A) Vessel network staining in brown was localized at the periphery of the tumor. Blood vessels in the periphery (B) and the centre of the tumor (C, D) were also stained with CD160 mAb, whereas tumor cells remained unstained. Magnification, 400 x.

**Figure 7. sHLA-G1 binds to the CD160 receptor expressed by endothelial cells.** (A) Left profiles: anti-CD160 mAb (open profile) stains Jurkat-CD160 but not untransfected Jurkat (black profiles, isotype control): flow cytometry analysis. Right profiles: sHLA-G1 tetramer binds to HUVEC and Jurkat-CD160 control transfectant (open profiles) but not to untransfected Jurkat cells (black profiles, control staining with streptavidin-PE): flow cytometry analysis. (B) Recombinant sHLA-G1 (sG1) blocks CD160 mAb binding to HUVEC (black profile, isotype control): flow cytometry analysis. Results are representative of 3 independent experiments. (C) Soluble CL1-R2 anti-CD160 mAb triggers inhibition of *in vitro* angiogenesis. HUVEC were seeded on Matrigel in the presence or absence of FGF2 (10 ng/mL) and sHLA-G1 (sG1, 1  $\mu$ g/mL) and/or CD160 mAb (+++, 10  $\mu$ g/mL; +, 1  $\mu$ g/mL) or IgG1-isotype control (10  $\mu$ g/mL). Photographs of each well were taken after 24 hours and angiogenesis quantified. Results are mean  $\pm$  SD of triplicate wells and are representative of 5 independent experiments. \*\*\* $P$  < 0.001, \* $P$  < 0.005, ns, not significant, ANOVA test, compared to FGF2-treated cells. (D) Soluble CL1-R2 anti-CD160 mAb induces HUVEC but not fibroblast apoptosis. HUVEC were either treated with sG1 (1  $\mu$ g/mL), CD160 mAb (10  $\mu$ g/mL), or control IgG1 (10  $\mu$ g/mL) or untreated (UT) for 50 hours in the presence of VEGF (50 ng/mL). Apoptotic cells were detected by flow cytometry using Annexin V/PI double staining (left-hand side panel, representative experiment). Right hand-side histograms: data are shown as mean percentage of Annexin V positive cells of 3 different experiments  $\pm$  SEM. \* $P$   $\leq$  0.02, Student t test.

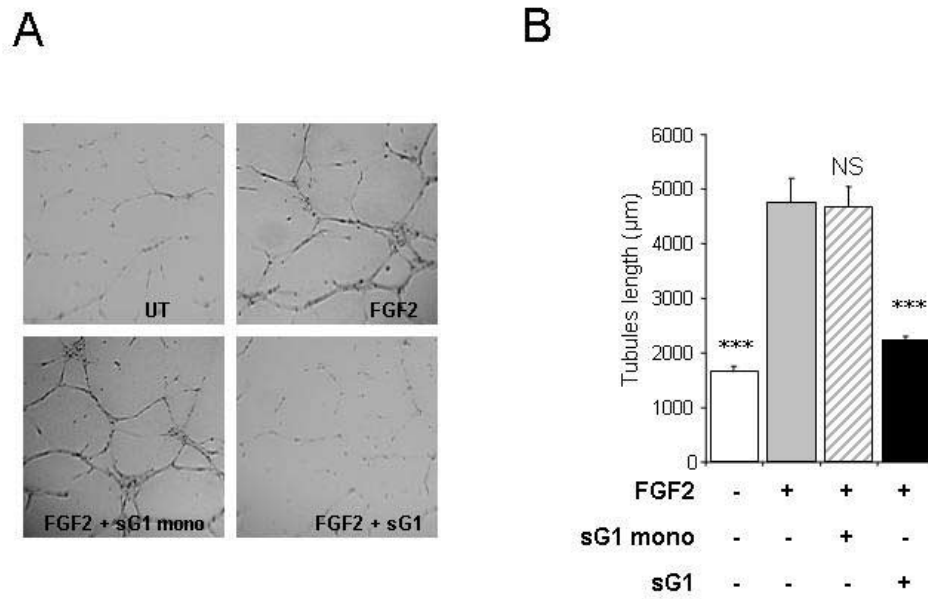


Figure 1

Fons et al.

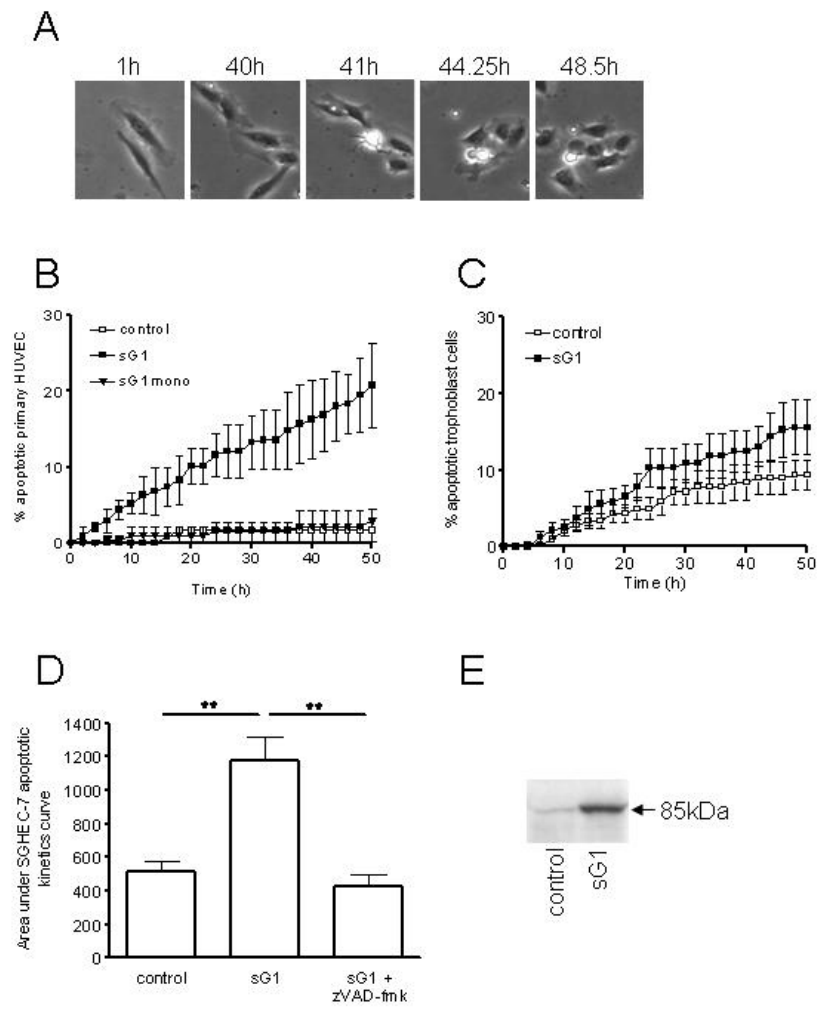
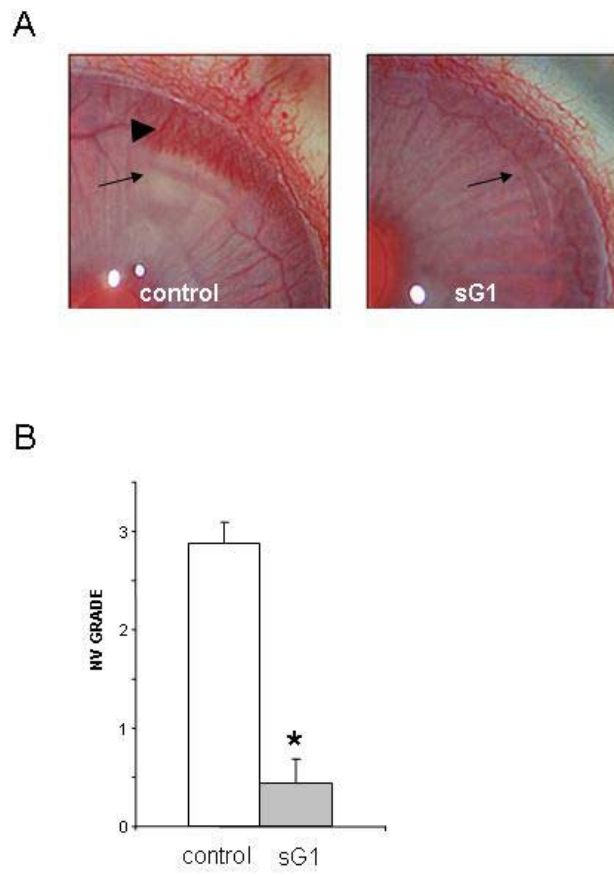


Figure 2



**Figure 3**

Fons et al.

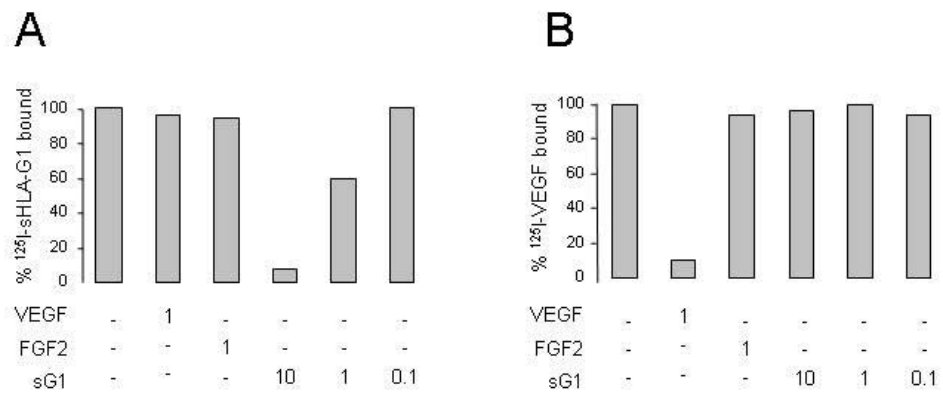
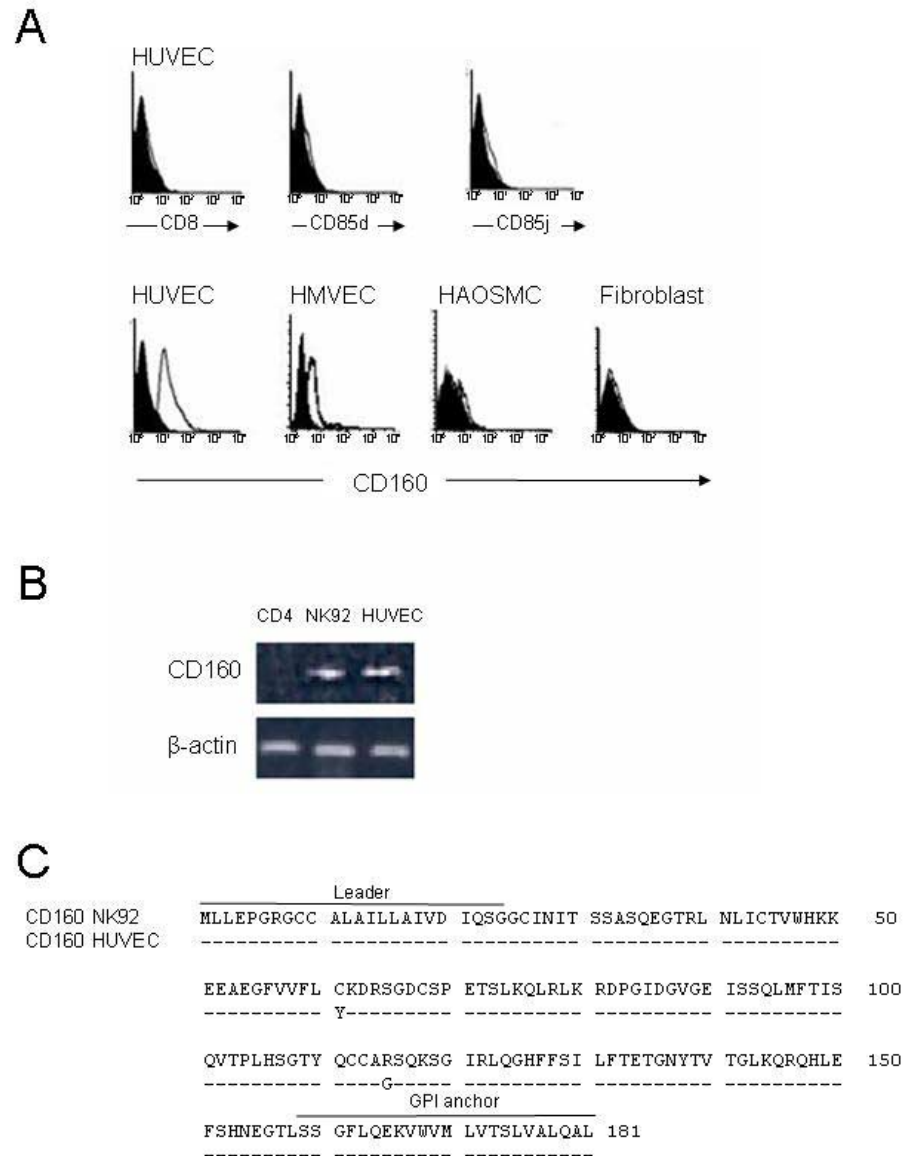


Figure 4

Fons et al.



**Figure 5**

Fons et al.

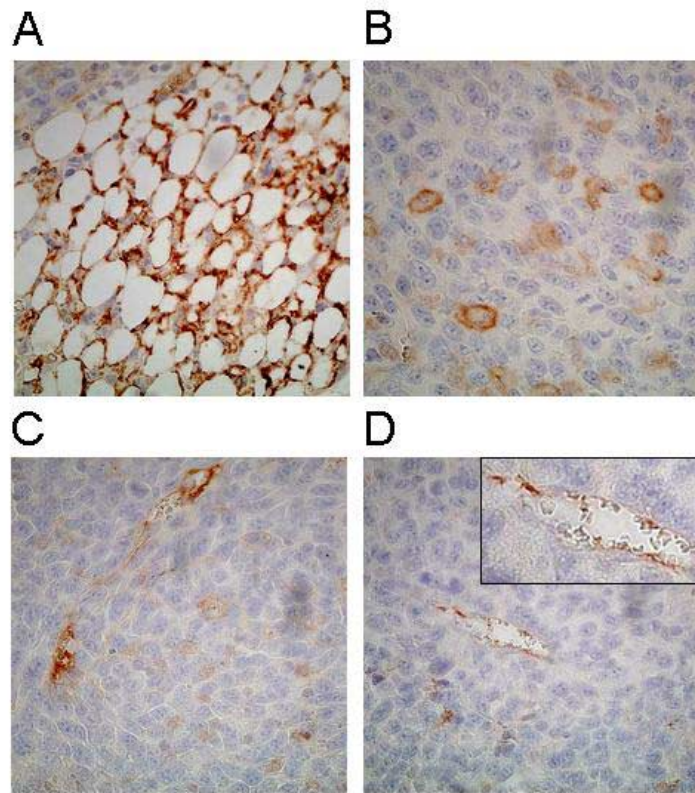


Figure 6

Fons et al.





**blood**<sup>®</sup>

Prepublished online June 29, 2006;  
doi:10.1182/blood-2005-12-019919

## **Soluble HLA-G1 inhibits angiogenesis through an apoptotic pathway and by direct binding to CD160 receptor expressed by endothelial cells**

Pierre Fons, Sophie Chabot, Judith E Cartwright, Françoise Lenfant, Fatima L'Faqihi, Jerome Giustiniani, Jean-Pascal Hérault, Genevieve Gueguen, Françoise Bono, Pierre Savi, Maryse Aguerre-Girr, Sylvie Fournel, François Malecaze, Armand Bensussan, Jean Plouet and Philippe Le Bouteiller

---

Information about reproducing this article in parts or in its entirety may be found online at:  
[http://www.bloodjournal.org/site/misc/rights.xhtml#repub\\_requests](http://www.bloodjournal.org/site/misc/rights.xhtml#repub_requests)

Information about ordering reprints may be found online at:  
<http://www.bloodjournal.org/site/misc/rights.xhtml#reprints>

Information about subscriptions and ASH membership may be found online at:  
<http://www.bloodjournal.org/site/subscriptions/index.xhtml>

---

Advance online articles have been peer reviewed and accepted for publication but have not yet appeared in the paper journal (edited, typeset versions may be posted when available prior to final publication). Advance online articles are citable and establish publication priority; they are indexed by PubMed from initial publication. Citations to Advance online articles must include digital object identifier (DOIs) and date of initial publication.